Mixed Valency

DOI: 10.1002/anie.200702760

Observation of Three Intervalence-Transfer Bands for a Class II–III Mixed-Valence Complex of Ruthenium**

Reginaldo C. Rocha, Francisca N. Rein, Hershel Jude, Andrew P. Shreve, Javier J. Concepcion, and Thomas J. Meyer**

Mixed valency in metal complexes such as the Creutz–Taube ion[1,2] $[(NH_3)_5Ru^{II}(\mu\text{-pz})Ru^{III}(NH_3)_5]^{5+}$ (**1**; pz = pyrazine) has been investigated for over forty years,[2–7] although a major remaining challenge is to develop a detailed understanding of the localized-to-delocalized transition (that is, Class II to Class III in the Robin–Day classification scheme).[4–6,8] A useful probe for assessing the extent of electronic delocalization has come from analysis of the intervalence-transfer (IT) absorption bands that typically appear in the near-IR spectra.[2,3,5,6] In the valence-localized limit, these IT bands arise from photoinduced intramolecular electron transfer across the ligand bridging the mixed-valence centers, that is, $M^n\text{-L-}M^{n+1} \xrightarrow{h\nu} M^{n+1}\text{-L-}M^n$.

A semi-classical theoretical treatment of electronic coupling and localization versus delocalization was provided by Hush.[3] This treatment was based on the average-mode approximation and assumed a single orbital interaction. However, the multiple ligand-mediated orbital interactions in transition-metal complexes, such as **1**, can result in multiple IT transitions split by low symmetry and spin-orbit coupling.[5] For $d\pi^6$–$d\pi^5$ systems, in particular, this is predicted to give rise to five low-energy transitions, three of IT origin and two of interconfigurational (IC) origin, as depicted in Figure 1.

Neglecting the reorganization energy for the IC transitions, the IT band energies are related by $E_{IT(1)} = \lambda$, $E_{IT(2)} \approx E_{IT(1)} + E_{IC(1)}$, and $E_{IT(3)} \approx E_{IT(1)} + E_{IC(2)}$, where λ is the reorganization energy for the bridge-mediated electron transfer. The IC band energies $E_{IC(1)}$ and $E_{IC(2)}$ depend on the local symmetry at M^{III} and the magnitude of the spin-orbit coupling constant ζ.[5] Only the lowest-energy IT(1) absorption arises from electron transfer in the ground state—the higher-energy IT(2) and IT(3) absorptions lead to IC excited states at the donor site and are of mixed IT/IC character.

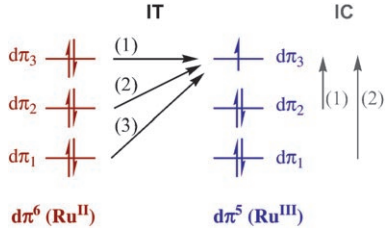

Figure 1. IT and IC transitions in d^6–d^5 mixed-valence systems such as Ru^{II}-L-Ru^{III} complexes.

The predicted spectral pattern of five low-energy bands has been observed in the near-IR/IR regions for mixed-valence Os dimers[5,9] in Class II–III.[5] Although valences (oxidation states) are localized in this intermediate class, electron transfer between the metal sites is sufficiently rapid that solvent is averaged and no longer contributes to λ. As a consequence, the decreased band energies and widths result in well separated IT absorptions for Os systems, where the large spin-orbit coupling constant of Os^{III} ($\zeta \approx 3000\ cm^{-1}$) increases the energy spacings for both IT and IC transitions.

Although the model is generally applicable to d^6–d^5 systems, there is limited evidence for analogous behavior in complexes of Ru or Fe, for which the decreased magnitudes of the spin-orbit coupling ($\zeta(Ru^{III}) \approx 1000\ cm^{-1}$; $\zeta(Fe^{III}) \approx 400$–$500\ cm^{-1}$) lead to closely spaced IT bands with overlapping absorptions as well as IC bands that are shifted into the IR and have greatly reduced absorptivities (which vary as the square of the spin-orbit coupling constant[5]).

Herein we report an experimental demonstration of multiple IT absorption bands for $[Cl_3Ru^{II}(tppz)Ru^{III}Cl_3]^-$ (**2**$^-$; tppz = 2,3,5,6-tetrakis(2-pyridyl)pyrazine), a green complex whose structural and electronic features reveal Class II–III mixed-valence behavior.

The anionic complex **2**$^-$ was prepared and isolated as salts of PPN (bis(triphenylphosphoranylidene)ammonium) or TBA (tetra(*n*-butyl)ammonium) cations. As observed in analogous complexes,[10] its crystal structure[11] (Figure 2) reveals a significant distortion from planarity in the tppz bridge, which adopts a saddle-like geometry with pyridyl groups alternately displaced upward and downward around the pyrazine ring (the torsion angle between adjacent pyridyl rings is around 20°). Relevant in this case is the finding that

[*] Dr. R. C. Rocha, Dr. H. Jude, Dr. A. P. Shreve
Center for Integrated Nanotechnologies, Materials Physics and Applications Division, Los Alamos National Laboratory
Mail Stop G755, Los Alamos, NM 87545 (USA)
Fax: (+1) 505-665-9030
E-mail: rcrocha@lanl.gov
Dr. J. J. Concepcion, Dr. T. J. Meyer
Department of Chemistry, University of North Carolina
Chapel Hill, NC 27599-3290 (USA)
Fax: (+1) 919-962-2388
E-mail: tjmeyer@unc.edu
Dr. F. N. Rein
Physical Chemistry and Applied Spectroscopy, Chemistry Division, Los Alamos National Laboratory
Los Alamos, NM 87545 (USA)

[**] This work was supported by the UCDRD program (at LANL) and the NSF (at UNC; grant CHE554561). The assistance of Dr. S. Iyer (mass spectrometry) is gratefully acknowledged.

Supporting information for this article (UV/Vis and ESI mass spectra, electrochemical data, and additional near-IR/IR spectra) is available on the WWW under http://www.angewandte.org or from the author.

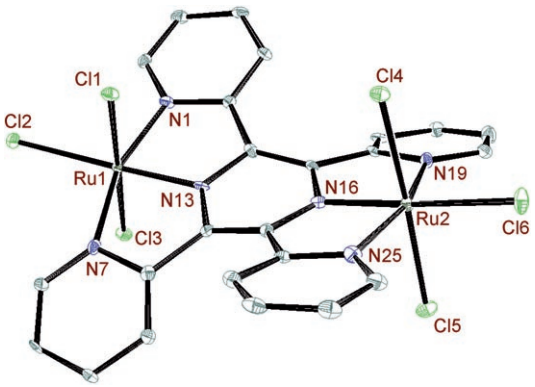

Figure 2. X-ray crystal structure of the mixed-valence complex $[Cl_3Ru(tppz)RuCl_3]^-$ ($\mathbf{2}^-$). H atoms and the counterion (PPN) are omitted for clarity.[11]

the coordination environments are *not* equivalent across the bridge, as shown by the metal–ligand bond lengths (Ru1–N13 1.940(4), Ru1–N1 2.071(5), Ru1–N7 2.066(5), Ru1–Cl2 2.392(14), Ru2–N16 1.912(4), Ru2–N19 2.059(5), Ru2–N25 2.041(5), and Ru2–Cl6 2.430(13) Å). The structure is consistent with valence localization in the solid state, with Ru1 as Ru^{III} and Ru2 as Ru^{II}.[12] The rather short Ru–N(pz) distances relative to the Ru–N(py) distances reflect the strong electron-acceptor ability of the bridging pyrazine (which promotes the metal–metal electronic coupling) as well as the overall structural constraints of the tppz bridge. The geometric distance between Ru1 and Ru2 is 6.504 Å.

The electrochemical oxidation and reduction of the $\mathbf{2}^-$ ion into its isovalent neutral ($\mathbf{2}^{\mathbf{0}}$; Ru^{III}–Ru^{III}) and dianionic ($\mathbf{2}^{\mathbf{2-}}$; Ru^{II}–Ru^{II}) forms are fully reversible and occur at 0.38 and −0.33 V vs. Ag/Ag^+ in acetonitrile and at 0.30 and −0.45 V vs. Ag/Ag^+ in dmf, respectively.[13] The large $\Delta E_{1/2}$ values (710 mV in acetonitrile and 750 mV in dmf) point to extensive electronic delocalization and stabilization of the mixed-valence state relative to the isovalent states, as reflected by comproportionation constants[14] (K_c) of the order of 10^{12} for the corresponding redox equilibrium [Eq (1)].

$$\{Ru^{II} - Ru^{II}\} + \{Ru^{III} - Ru^{III}\} \xrightleftharpoons{K_c} 2\{Ru^{II} - Ru^{III}\} \quad (1)$$

Three absorption bands appear in the near-IR/IR spectrum of $\mathbf{2}^-$ (Figure 3a). These can be assigned to the three IT transitions shown in Figure 1, with E_{IT} ($\tilde{\nu}_{max}$) values of 5560 cm^{-1}(ε=3500 $M^{-1}cm^{-1}$; full width at half maximum (FWHM) = 1150 cm^{-1}), 3300 cm^{-1} (ε = 1200 $M^{-1}cm^{-1}$; FWHM = 1050 cm^{-1}), and 2200 cm^{-1} (ε = 250 $M^{-1}cm^{-1}$; FWHM = 800 cm^{-1}) for IT(3), IT(2), and IT(1), respectively.[15] $E_{IC(1)}$ and $E_{IC(2)}$ are predicted from these IT band energies to appear at approximately 1100 and 3360 cm^{-1}. A putative IC(1) band does appear at 1200–1600 cm^{-1}, but it is of low absorptivity (< 200 $M^{-1}cm^{-1}$) and is overlaid by the vibrational peaks in this IR region. The assignments of these bands were confirmed by differential spectroelectrochemistry.

As shown in the differential near-IR/IR spectrum in Figure 3b, in situ spectroelectrochemical oxidation of $\mathbf{2}^-$

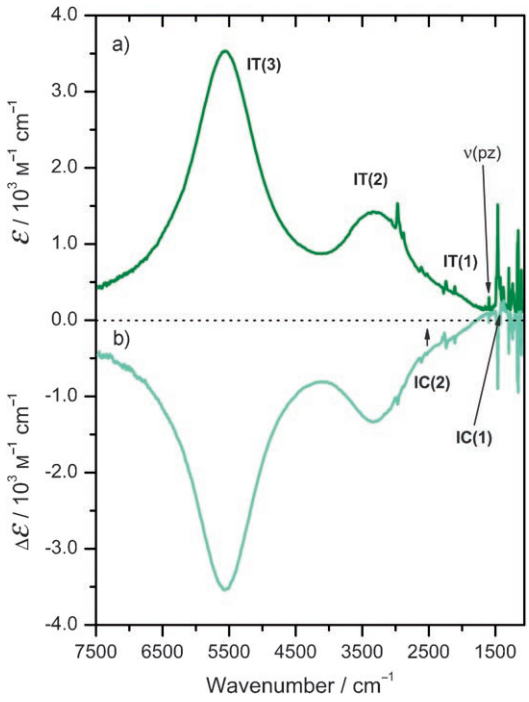

Figure 3. a) Near-IR/IR spectra of the $\mathbf{2}^-$ anion and b) difference near-IR/IR spectra of $\mathbf{2}^{\mathbf{0}}$ upon in situ oxidation of $\mathbf{2}^-$ (reference) in CD_3CN.[13]

(Ru^{II}–Ru^{III}) into $\mathbf{2}^{\mathbf{0}}$ (Ru^{III}–Ru^{III}) results in the loss of all three IT bands. Also observed in the difference spectrum is a new feature that evolves below 2000 cm^{-1} ($\tilde{\nu}_{max} \approx 1440$ cm^{-1}; $\Delta\varepsilon \approx 250$ $M^{-1}cm^{-1}$; FWHM ≈ 450 cm^{-1})[15] for which the enhanced absorptivity upon oxidation of $d\pi^5$–$d\pi^6$ (Ru^{II}–Ru^{III}) to $d\pi^5$–$d\pi^5$ (Ru^{III}–Ru^{III}) is consistent with an IC assignment. A similar comparative analysis of Figures 3b and 3a reveals a relative increase in absorptivity from 2000 to 3000 cm^{-1} for $\mathbf{2}^{\mathbf{0}}$ ($\tilde{\nu}_{max} \approx 2600$ cm^{-1}; $\Delta\varepsilon < 150$ $M^{-1}cm^{-1}$; FWHM > 500 cm^{-1}),[15] which is consistent with IC(2). The IC(2) absorption in the spectrum of $\mathbf{2}^-$ is hidden between the IT(1) and IT(2) bands.

As expected in Class II–III,[5] the IT bands for $\mathbf{2}^-$ appear at low energy, have narrow bandwidths, and are independent of solvent.[13] For comparison, for the cation $[(bpy)_2ClRu^{II}(\mu\text{-}pz)Ru^{III}Cl(bpy)_2]^{3+}$, which is a fully localized complex in Class II, a single solvent-dependent, unresolved broad band is observed at 7690 cm^{-1} in CD_3CN with a FWHM ($\Delta\tilde{\nu}_{1/2}$) of about 4000 cm^{-1}.[16] The narrowness of the IT bands for $\mathbf{2}^-$ is illustrated by comparing the observed bandwidths (i.e. FWHM) with the theoretically estimated values, which gives $\Delta\tilde{\nu}_{1/2}(exp)/\Delta\tilde{\nu}_{1/2}(calc)$ ratios (where $\Delta\tilde{\nu}_{1/2}(calc) = [16RT\tilde{\nu}_{max}\ln(2)]^{1/2}$)[3] of 0.35 ± 0.02. Such narrow bandwidths are consistent with rapid electron transfer and valence averaging on the time scale of solvent motions (i.e., a negligible contribution of solvent to λ). Additional evidence for solvent averaging in $\mathbf{2}^-$ comes from the solvent insensitivity of the bridge-based metal-to-ligand charge transfer (MLCT; $Ru^{II} \rightarrow \pi^*_{tppz}$) absorption band at 660 nm ($\varepsilon = 2 \times 10^4$ $M^{-1}cm^{-1}$).[13]

Localization/delocalization on the time scale of intramolecular vibrational motions can be probed by the presence/absence of IR activity in symmetric vibrations of bridging ligands.[5] Thus, the peak at 1596 cm^{-1} ($\varepsilon \approx 300\ M^{-1}\,cm^{-1}$) in Figure 3a originates from a symmetric pyrazine ring stretch in tppz (analogous to the ν_{8a} mode of unsubstituted pyrazine[17]) and its appearance is consistent with local electronic asymmetry owing to valence localization in $\mathbf{2}^-$.

The spectral features observed for $\mathbf{2}^-$ provide an interesting comparison with those deduced for **1**,[5] where $E_{IT(1)} = 4500–5000$, $E_{IT(2)} = 6320$, $E_{IT(3)} = 7360$, $E_{IC(1)} = 2000$, and $E_{IC(2)} = 3200\ cm^{-1}$. The assignment of the lowest-energy IT band to a $d_\delta(Ru^{II}) \rightarrow d_\pi(Ru^{III})$ transition (with $d_\delta(Ru^{II})$, to zero order, orthogonal to the bridge) is consistent with the pattern of absorptivities ($\varepsilon_{IT(1)} \ll \varepsilon_{IT(2)}, \varepsilon_{IT(3)}$) found in both cases. As with $\mathbf{2}^-$, the appearance of an IR peak for the symmetric bridging ν_{8a}(pz) mode in **1** provides evidence for electronic symmetry breaking on the time scale of the vibrational period (approximately 20 fs).[5]

The results described herein are important in providing, direct evidence for multiple IT transitions in a mixed-valence complex of ruthenium. The predicted five-band pattern is applicable to $\mathbf{2}^-$ with discernible, resolved IT absorption bands because the solvent does not contribute to band energies and widths. The underlying model provides a systematic basis for analyzing Class II–III and probing localization-to-delocalization in transition-metal complexes.

Experimental Section

Materials: Ruthenium(III) trichloride hydrate, tetra(2-pyridyl)pyrazine (tppz), PPNCl (PPN = bis(triphenylphosphoranylidene)ammonium), and TBACl (TBA = tetra(*n*-butyl)ammonium) were used as supplied. Organic solvents were analytical high-purity grade and were used as received. Solvents used in the preparation of solutions for electrochemical/spectroscopic experiments were dried and stored over 4-Å molecular sieves. $[N(nBu)_4]PF_6$ (TBAH) was recrystallized twice from absolute ethanol and dried in vacuo prior to its use as the supporting electrolyte in solutions for electrochemical experiments.

$[(EtOH)Cl_2Ru^{II}(tppz)Ru^{III}Cl_3]$: A solution of ruthenium(III) trichloride hydrate (1.5 g, 5.74 mmol) and tppz (0.76 g, 1.95 mmol) in ethanol (350 mL) was heated under reflux for 18 h in air and then cooled to room temperature. The solid product was collected by filtration, washed with ethanol (50 mL) and diethyl ether (150 mL), and dried under vacuum. Yield: 1.55 g (97%).

$PPN[Cl_3Ru^{II}(tppz)Ru^{III}Cl_3]$: A mixture of $[(EtOH)Cl_2Ru^{II}(tppz)Ru^{III}Cl_3]$ (0.5 g, 0.61 mmol) and PPNCl (6.1 g, 10.6 mmol) in acetone (200 mL) was heated under reflux for 3 h and then cooled to room temperature. The solid was collected by filtration, washed with acetone (100 mL) and diethyl ether (100 mL), and dried under vacuum. Yield: 0.75 g (91%). Crystals suitable for X-ray structural determination were grown from acetonitrile solution.

$TBA[Cl_3Ru^{II}(tppz)Ru^{III}Cl_3]$: A mixture of $[(EtOH)Cl_2Ru^{II}(tppz)Ru^{III}Cl_3]$ (0.6 g, 0.74 mmol) and TBACl (3.5 g, 12.7 mmol) in acetone 300 mL was heated under reflux for 3 h. After cooling to room temperature, the solution was poured into diethyl ether (200 mL). The precipitate was collected by filtration, washed with diethyl ether (100 mL), and vacuum-dried. Yield: 0.55 g (71%).

$[Cl_3Ru^{III}(tppz)Ru^{III}Cl_3]$: The isovalent, neutral complex $[Cl_3Ru^{III}(tppz)Ru^{III}Cl_3]$ was isolated by chemical oxidation of $[Cl_3Ru^{II}(tppz)Ru^{III}Cl_3]^-$ in acetonitrile with Ce^{IV} (as $(NH_4)_2Ce(NO_3)_6$; 1.1 equiv) followed by precipitation into diethyl ether (typical yield: > 94%). This species could also be generated in situ by electrolysis of the isolated mixed-valence compound in acetonitrile solution (see details of the spectroelectrochemical experiments below).

$[Cl_3Ru^{II}(tppz)Ru^{II}Cl_3]^{2-}$: Although the mixed-valence Ru^{II}–Ru^{III} and fully oxidized Ru^{III}–Ru^{III} species are chemically stable in solution or the solid state, their fully reduced Ru^{II}–Ru^{II} counterpart is only stable within the time scale of the electrochemical experiments and undergoes slow substitution of chloride to give a solvent-coordinated species.

Electrospray ionization (ESI) mass spectra were recorded with a QStar XL instrument (Applied Biosystems) equipped with a Protana Nanospray source. Data were acquired in TOF-MS mode using standard voltage parameters for m/z in the range 400–1500 and processed using the Analyst software. UV/Vis absorption spectra were recorded with a Cary 300 spectrophotometer. A BAS CV-50W potentiostat (Bioanalytical Systems) was used in electrochemical experiments. For cyclic voltammetry, a conventional three-electrode setup consisting of a Pt disk (1.6 mm) as the working electrode, a coil of Pt wire as the auxiliary electrode, and an Ag wire immersed in a CH_3CN solution containing 0.010 M $AgNO_3$ and 0.10 M TBAH as the reference electrode. The sample solutions were thoroughly deoxygenated with a stream of argon prior to each measurement. The voltammograms were recorded at sweep rates of 10–1000 $mV\,s^{-1}$. Potentials are referenced to Ag/Ag^+ at room temperature.

Near-IR and IR spectroscopic measurements of solution samples were performed with a Bruker Equinox 55 Fourier transform instrument. Data were collected under an atmosphere of dry nitrogen at a nominal resolution of 1 cm^{-1} (each spectrum is an average of 32 scans) at room temperature. Anhydrous deuterated solvents were used to prepare solutions with a concentration of about 5 mM. Spectroelectrochemical measurements in situ were carried out using an optically transparent thin-layer electrochemical cell with an internal optical path length of 100 μm (Teflon spacer) between the CaF_2 cell windows and a three-electrode system (with an Au minigrid as the optically transparent working electrode). The spectra of the isovalent species were obtained by controlled-potential electrolysis of the isolated, mixed-valence Ru^{II}–Ru^{III} species. The chemical stability and electrochemical reversibility were verified by spectral recovery in reversed oxidative/reductive steps. Curve-fitting analysis and spectral deconvolution were conducted by using the Peak Fitting Module subroutine of OriginPro 7.5 (OriginLab).

Received: June 22, 2007
Revised: August 10, 2007
Published online: December 3, 2007

Keywords: charge transfer · electron transfer · IR spectroscopy · mixed-valent compounds · ruthenium

[1] C. Creutz, H. Taube, *J. Am. Chem. Soc.* **1969**, *91*, 3988.
[2] C. Creutz, *Prog. Inorg. Chem.* **1983**, *30*, 1.
[3] N. S. Hush, *Prog. Inorg. Chem.* **1967**, *8*, 391.
[4] M. B. Robin, P. Day, *Adv. Inorg. Chem.* **1967**, *10*, 247.
[5] K. D. Demadis, C. M. Hartshorn, T. J. Meyer, *Chem. Rev.* **2001**, *101*, 2655.
[6] B. S. Brunschwig, C. Creutz, N. Sutin, *Chem. Soc. Rev.* **2002**, *31*, 168; D. M. D'Alessandro, F. R. Keene, *Chem. Soc. Rev.* **2006**, *35*, 424.
[7] W. Kaim, G. K. Lahiri, *Angew. Chem.* **2007**, *119*, 1808; *Angew. Chem. Int. Ed.* **2007**, *46*, 1778.
[8] S. F. Nelsen, *Chem. Eur. J.* **2000**, *6*, 581.
[9] K. D. Demadis, G. A. Neyhart, E. M. Kober, P. S. White, T. J. Meyer, *Inorg. Chem.* **1999**, *38*, 5948; K. D. Demadis, E. S. El-Samanody, G. M. Coia, T. J. Meyer, *J. Am. Chem. Soc.* **1999**, *121*, 535.
[10] C. M. Hartshorn, N. Daire, V. Tondreau, B. Loeb, T. J. Meyer, P. S. White, *Inorg. Chem.* **1999**, *38*, 3200.

[11] CCDC 651711 contains the supplementary crystallographic data for this paper. These data can be obtained free of charge from The Cambridge Crystallographic Data Centre via www.ccdc.cam.ac.uk/data_request/cif.
[12] D. S. Eggleston, K. A. Goldsby, D. J. Hodgson, T. J. Meyer, *Inorg. Chem.* **1985**, *24*, 4573.
[13] See the Supporting Information.
[14] D. E. Richardson, H. Taube, *Coord. Chem. Rev.* **1984**, *60*, 107.
[15] As determined by spectral deconvolution and lineshape analysis.
[16] R. W. Callahan, F. R. Keene, T. J. Meyer, D. J. Salmon, *J. Am. Chem. Soc.* **1977**, *99*, 1064.
[17] R. C. Rocha, A. P. Shreve, *Inorg. Chem.* **2004**, *43*, 2231; R. C. Rocha, M. G. Brown, C. H. Londergan, J. C. Salsman, C. P. Kubiak, A. P. Shreve, *J. Phys. Chem. A* **2005**, *109*, 9006; R. C. Rocha, A. P. Shreve, *Chem. Phys.* **2006**, *326*, 24.

